Eur. Phys. J. B **25**, 463–478 (2002)
DOI: 10.1140/epjb/e20020052

THE EUROPEAN PHYSICAL JOURNAL B
EDP Sciences

Ursell operators in statistical physics of dense systems: the role of high order operators and of exchange cycles

J.N. Fuchs, M. Holzmann[a], and F. Laloë[b]

Laboratoire Kastler Brossel[c], Département de Physique de l'ENS, 24 rue Lhomond, 75005 Paris, France

Received 18 October 2001

Abstract. The purpose of this article is to discuss cluster expansions in dense quantum systems, as well as their interconnection with exchange cycles. We show in general how the Ursell operators of order $l \geq 3$ contribute to an exponential which corresponds to a mean-field energy involving the second operator U_2, instead of the potential itself as usual – in other words, the mean-field correction is expressed in terms of a modification of a local Boltzmann equilibrium. In a first part, we consider classical statistical mechanics and recall the relation between the reducible part of the classical cluster integrals and the mean-field; we introduce an alternative method to obtain the linear density contribution to the mean-field, which is based on the notion of tree-diagrams and provides a preview of the subsequent quantum calculations. We then proceed to study quantum particles with Boltzmann statistics (distinguishable particles) and show that each Ursell operator U_n with $n \geq 3$ contains a "tree-reducible part", which groups naturally with U_2 through a linear chain of binary interactions; this part contributes to the associated mean-field experienced by particles in the fluid. The irreducible part, on the other hand, corresponds to the effects associated with three (or more) particles interacting all together at the same time. We then show that the same algebra holds in the case of Fermi or Bose particles, and discuss physically the role of the exchange cycles, combined with interactions. Bose condensed systems are not considered at this stage. The similarities and differences between Boltzmann and quantum statistics are illustrated by this approach, in contrast with field theoretical or Green's functions methods, which do not allow a separate study of the role of quantum statistics and dynamics.

PACS. 05.30.-d Quantum statistical mechanics – 05.20.Jj Statistical mechanics of classical fluids

1 Introduction

A widely used formalism in quantum statistical physics is the formalism of Green's functions [1–3], where the techniques of second quantization and field theory are used from the beginning; the notion of exchange operators of indistinguishable particles is of course contained, but in a completely implicit way. In the formalism of Ursell operators [4–6], the starting point is first quantization with numbered particles, so that the role of exchange cycles becomes completely explicit: these cycles appear clearly in all diagrams and, for instance, they are the only source of diagrams for the ideal quantum gas. This reduces the distance between the formalism and, for instance, numerical calculations such as the PIMC method (Path Integral Monte Carlo), where particles are also numbered and the exchange cycles are explicitly sampled by random choices. Moreover, it becomes possible to assume that the particles obey Boltzmann statistics, just by "switching off the cycles", a task that would be difficult in the Green's function formalism. Needless to say, this does not mean that Green's functions are, in general, less powerful than the Ursell formalism! The opposite is actually closer to reality: for instance, Green's functions handle time-dependent problems easily, while this is not the case in the Ursell formalism. But it remains true that, if one is interested in a detailed discussion of the effects of quantum statistics at equilibrium, it becomes more straightforward to resort to the Ursell formalism.

In this article, we consider dense systems, for which it is not necessarily possible to limit oneself to first order density effects. In contrast to the situation in a dilute gas, a given particle may interact frequently with several others at the same time, and even liquefaction may take place. Therefore, we will no longer ignore all Ursell operators beyond U_2, as was done in most of previous work in this formalism; operators U_3, U_4, etc. now become important.

[a] *Present address:* Physics Department, University of Illinois at Urbana-Champaign, 1110 W. Green St., Urbana, Il 61801, USA

[b] e-mail: `franck.laloe@lkb.ens.fr`

[c] The "Laboratoire Kastler Brossel (LKB)" is "Unité Mixte de Recherche du CNRS (UMR 8552) et de l'Université Pierre et Marie Curie (Paris)".

One may actually wonder what the role of these higher order operators is in general, and why exactly it is possible to ignore their role in a dilute system, as was done in [6] for instance. We will see that part of their contribution (what we will call their tree reducible part) groups naturally with U_2 through a chain of binary interactions, and builds an exponential of the mean-field energy. In other words, instead of making the problem more complicated, this contribution of the higher order operators builds exactly the exponential of U_2 that is needed to reconstruct a simple and natural expression of the mean-field. Nevertheless, this mean-field is expressed in terms of the matrix elements of U_2, instead of the usual matrix elements of the potential itself; in a sense, what we obtain is the exponential of an exponential, since U_2 itself contains exponentials of the Hamiltonian and corresponds physically to the local change of the Boltzmann equilibrium. As a consequence, the logarithms that appeared in [6], and had to be expanded to first order in density, are actually spurious – in other words, this first order expansion was actually unnecessary. In addition, the rest of the contribution of the higher order Ursell operators, the irreducible part, vanishes unless three particles (or more) are all close together, and is really characteristic of many-body collisions and of dense systems.

2 Classical statistical physics

In this part, we quickly review the classical cluster expansion for the parametric equation of state of a fluid; we first recall the results of classical statistical mechanics as a point of comparison.

2.1 General formalism

The general expression of the equation of state was derived by Mayer [7] and Ursell [8]; see also the books by Uhlenbeck and Ford [9] and Hansen and McDonald [10]. A classical system of massive particles, with mass m, is supposed to be contained in a box of finite volume $\mathcal{V}$, with periodic boundary conditions (translationally invariant system); their Hamiltonian is the sum of the kinetic energies plus the interaction energy, which is the sum over all pairs of particles of the interparticle pair potential $V_{ij} = V(\mathbf{r_i} - \mathbf{r_j})$. An useful function in the calculation is the Mayer function f_{ij} defined by:

$$f_{ij} \equiv \exp(-\beta V_{ij}) - 1. \tag{1}$$

This function is everywhere bounded and goes to almost zero when the distance between particles i and j is much larger than the range of the pair potential; it is the classical equivalent of a second Ursell operator $\overline{U}_2(i,j)$ [6].

The classical cluster expansion is the expansion, in the grand canonical ensemble, of the pressure p and of the density ρ of the gas in series of the fugacity $z = \mathrm{e}^{\beta\mu}$, where μ is the chemical potential and $\beta = 1/k_{\mathrm{B}}T$ is the inverse temperature. If λ is the de Broglie thermal wavelength, the expansion can be written as:

$$\beta p = \frac{\ln Z_{\mathrm{gc}}}{\mathcal{V}} = \sum_{l=1}^{\infty} b_l(T,\mathcal{V}) \left(\frac{z}{\lambda^3}\right)^l \tag{2}$$

with:

$$\rho = \frac{\langle N\rangle}{\mathcal{V}} = z\frac{\partial}{\partial z}\left(\frac{\ln Z_{\mathrm{gc}}}{\mathcal{V}}\right) = \sum_{l=1}^{\infty} l\ b_l(T,\mathcal{V}) \left(\frac{z}{\lambda^3}\right)^l \tag{3}$$

where $Z_{\mathrm{gc}}(\beta,\mathcal{V},z)$ is the grand canonical partition function; the definition of the cluster integrals $b_l(T,\mathcal{V})$ is the same as that in the book of Mayer and Mayer [7]. The first coefficients are given by:

$$b_1(T,\mathcal{V}) = \frac{1}{1!\mathcal{V}} \int \mathrm{d}^3 r_1 = 1 \tag{4}$$

$$b_2(T,\mathcal{V}) = \frac{1}{2!\mathcal{V}} \int \mathrm{d}^3 r_1\, \mathrm{d}^3 r_2\ f_{12} = \frac{1}{2!} \int \mathrm{d}^3 r_{12}\ f(r_{12}) \tag{5}$$

$$b_3(T,\mathcal{V}) = \frac{1}{3!\mathcal{V}} \int \mathrm{d}^3 r_1\, \mathrm{d}^3 r_2\, \mathrm{d}^3 r_3 [f_{12}f_{13} + f_{12}f_{23} + f_{13}f_{23} + f_{12}f_{13}f_{23}] \tag{6}$$

and so on for $l \geq 4$; these definitions include a $1/\mathcal{V}$ factor so that $b_l(T,\mathcal{V})$ remains intensive when the volume tends to infinity.

It is useful to introduce diagrams to represent the integrals. A l-particle cluster diagram is made of l numbered circles, representing the particles, between which one draws any number of lines (also called links, and representing the f_{ij}'s), each line joining distinct pairs of circles. The diagram is said to be connected when one can go from any particle to any other particle in the cluster following the lines. The general definition of the cluster integrals is then:

$$b_l(T,\mathcal{V}) \equiv \frac{1}{l!\,\mathcal{V}} \times \text{sum over all possible } l\text{-particle clusters.} \tag{7}$$

For example:

$$b_1(T,\mathcal{V}) = \frac{1}{1!\mathcal{V}} (\ \bullet\ ) = 1 \tag{8}$$

$$b_2(T,\mathcal{V}) = \frac{1}{2!\mathcal{V}} (\bullet\!\!-\!\!\bullet) \tag{9}$$

and:

$$b_3(T,\mathcal{V}) = \frac{1}{3!\mathcal{V}} \left(\text{ 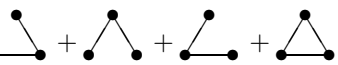 } \right). \tag{10}$$

2.2 Irreducible diagrams, energy shift and the equation of state

It turns out that, defined in this way, diagrams carry redundant information: as soon as $l \geq 3$, most of the diagrams contributing to b_l can be constructed as products of smaller diagrams (already contained in $b_{l'}$ with $l' < l$). For instance, this is the case of all diagrams in the right hand side of (10), except the last. It then becomes convenient to define the notion of irreducibility: an irreducible cluster is such that, if any line (which is essentially a b_2) is removed from it, it never splits into disconnected clusters; conversely, in a reducible cluster, it is possible to find at least one line that, when cut, will decompose the result into two separate clusters (since each line is essentially a b_2, reducibility and irreducibility are defined here in terms of binary coefficients b_2's, but more general definitions are conceivable).

Irreducible diagrams play a special role if one introduces an exponentiation of the fugacity expansion of the density (3). Let us define an energy shift Δ, which shifts all energy levels e_k, by the relation:

$$\rho = \mathrm{e}^{-\beta(\Delta-\mu)} \frac{1}{\lambda^3} \,. \tag{11}$$

It can then be shown (see [11–14]) that Δ is given by the series:

$$-\beta\Delta = \sum_{l=1}^{\infty} \beta_l(T,\mathcal{V})\, \rho^l \tag{12}$$

where the new coefficients β_l are defined by:

$$\beta_{l-1}(T,\mathcal{V}) \equiv \frac{1}{(l-1)!\mathcal{V}} \times \text{sum over all irreducible } l\text{-particle clusters} \tag{13}$$

or, equivalently:

$$\beta_{l-1}(T,\mathcal{V}) \equiv l \times \text{Irreducible part of } b_l(T,\mathcal{V}). \tag{14}$$

For example:

$$\beta_1(T,\mathcal{V}) = \frac{1}{\mathcal{V}} \left(\bullet\!\!-\!\!\bullet\right) = \int \mathrm{d}^3 r_{12}\ f(r_{12}) \tag{15}$$

and:

$$\beta_2(T,\mathcal{V}) = \frac{1}{2!\mathcal{V}} \left(\triangle\right). \tag{16}$$

One can also show that irreducible clusters are directly related to the equation of state (at finite volume), from which the variable z has been eliminated:

$$\frac{\beta p}{\rho} = 1 - \sum_{l=1}^{\infty} \frac{l}{l+1}\, \beta_l(T,\mathcal{V})\ \rho^l. \tag{17}$$

The proof of this result is given in the book by Mayer and Mayer [7]. Another method of calculation was introduced by Van Kampen [15], with the canonical ensemble instead of grand canonical; see also [16]. In these calculations, the thermodynamical limit is taken before the l summation while, here, we do not take this limit; the reason is that, as discussed by Lee and Yang [17], taking directly the limit for each coefficient reduces the validity of the calculation to the gaseous phase only.

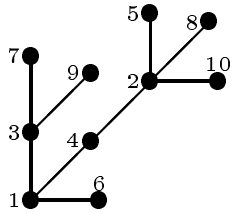

Fig. 1. A tree-diagram corresponding to a 10-particle cluster; the tree symbolizes one of the terms that are contained in the tree-reducible part of b_{10}. The construction method that is used to build the branches from the structure of the integral is explained in the text.

2.3 Tree-reducible diagrams; mean-field

Let us now suppose that, among all clusters contributing to b_l, we keep only those having l particles and $l-1$ links. They correspond to the minimally connected diagrams: if any link is removed, these diagrams split into two different diagrams. They are, not only obviously reducible (as soon as $l \geq 3$), but also "fully reducible", since the removal of any line splits the diagram into disconnected clusters. For instance, the fully reducible part of b_3 is:

$$b_3^{\mathrm{R}}(T) = \frac{1}{3!\mathcal{V}} \int \mathrm{d}^3 r_1\, \mathrm{d}^3 r_2\, \mathrm{d}^3 r_3 [f_{12} f_{13} + f_{12} f_{23} + f_{13} f_{23}] \tag{18}$$

from which the last term that appear on the right hand side of (6) has been eliminated. Graphically, we will represent these clusters by diagrams that have the structure of a tree, such as that of Figure 1, and for this reason we shall call them "tree-reducible diagrams".

In order to construct this tree-diagram, we have to choose one numbered particle as the "root particle", for instance particle 1. Then, among all particles j that are connected to particle 1 by a link f_{1j}, we select that with the smallest value of j; let us call k this particle. The same operation is then made again from particle k: one identifies the particle m to which it is related which has the smallest numbering, and puts this particle as the next in the branch; the same operation goes on until one reaches the end of the first branch, which is drawn vertically by convention. One then goes back along this branch towards the origin and identifies the first particle which is connected to another particle outside of the branch; this particle is a branching point, the source of another branch, which is built in exactly the same way, and drawn directly on the

right of the first branch. The same process continues and one adds successive branches, which are drawn in a clockwise order from their source; it stops when all particles are included in the tree. This construction provides a well defined geometry for the tree-diagram but, clearly, different tree-diagrams may have the same numerical value[1]. It is nevertheless convenient for our reasoning below to classify their contributions according to the various structures of trees.

For instance, the reducible part of b_3 then becomes:

$$b_3^{\mathrm{R}}(T,\mathcal{V}) = \frac{1}{3!}\left(2 \times \right. \qquad (19)$$

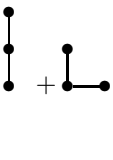

(from now on, we assume that the factor $1/\mathcal{V}$ is included in the value of the tree-diagram, in order to simplify the notation).

Let us now consider a given tree-diagram and evaluate its weight; the question is to determine how many different numberings are compatible with the rules that we have used to build it. Suppose then that we put random numbers into the $l-1$ nodes that are available in the tree. The result will be acceptable only if a correct clockwise ordering of the particle numbers is obtained at each bifurcation node. Let us call r_1, r_2, ... the branching factors (or ramification factors) of the nodes, *i.e.* the number of secondary branches at each node; a linear diagram has only $r = 1$, a diagram with one binary bifurcation has one $r = 2$, and r takes the values 3, 4, etc. when more branches start from the same source. Each node will then introduce a probability $1/r_i!$ for this correct ordering to be obtained. Since there are $(l-1)!$ ways of distributing the $l-1$ particles among the nodes, the final result is that the weight of the tree-diagram is:

$$\frac{(l-1)!}{\prod_i r_i!}\cdot \qquad (20)$$

If we call T_{diag} the value of a tree-diagram (including the $1/\mathcal{V}$ factor), we can then express the tree-reducible l particles cluster as:

$$l!\; b_l^{\mathrm{R}}(T) = \sum_{\{\text{tree diagrams}\}} \frac{(l-1)!}{\Pi_i(r_i)!}\, T_{\mathrm{diag.}} \qquad (21)$$

Inserting this expression into the z-expansion of the density (3), we notice that various simplifications take place in the coefficients, so that we obtain:

$$\rho = \frac{z}{\lambda^3}\left\{ 1 + \frac{z/\lambda^3}{1!} \times \right. \quad + \frac{(z/\lambda^3)^2}{2!}\left(\frac{2!}{2!} \times \right. \quad + \frac{2!}{1!} \times \quad \left.\right)$$

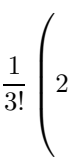

$$+ \ldots + \frac{(z/\lambda^3)^{l-1}}{(l-1)!} \times \frac{(l-1)!}{\Pi_i(r_i)!} \times \quad + \ldots \left.\right\}\cdot \qquad (22)$$

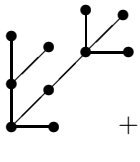

It is now possible to regroup diagrams according to the value of the branching factor r_1 at their root:

$$\rho = \frac{z}{\lambda^3}\left\{ 1 + \frac{1}{1!}\left[\frac{z}{\lambda^3} \right.\right. \quad + \left(\frac{z}{\lambda^3}\right)^2 \quad + \left(\frac{z}{\lambda^3}\right)^3 \quad + \ldots \left.\right]$$

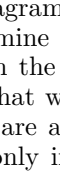

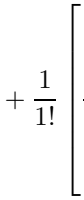

$$+ \frac{1}{2!}\left[\left(\frac{z}{\lambda^3}\right)^2 \quad + \ldots \right] + \ldots \left.\right\}\cdot \qquad (23)$$

One then notices a sort of self-similarity property of the expansion: at each secondary nodes, one gets an expansion that provides again all the terms that are contained in ρ. Therefore:

$$\rho = \frac{z}{\lambda^3}\left\{ 1 + \right. \quad + \frac{1}{2!} \times \quad + \ldots + \frac{1}{r_1!} \times \quad + \ldots \left.\right\}\cdot \qquad (24)$$

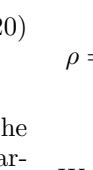

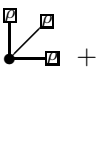

We now recognize the development of an exponential:

$$\rho = \frac{z}{\lambda^3}\left\{ 1 + \beta_1\rho + \frac{1}{2!} \times [\beta_1\rho]^2 + \ldots + \frac{1}{r_1!} \times [\beta_1\rho]^{r_1} + \ldots \right\}$$

where $\beta_1 = 2b_2$ is defined in (15), and finally obtain the very simple result:

$$\rho = \frac{z}{\lambda^3}\exp(\beta_1\rho) \qquad (25)$$

or:

$$-\beta\Delta = \beta_1\rho. \qquad (26)$$

[1] In fact, the value of these diagrams depends only on the total number of nodes (*i.e.* particles) l (see Appendix A).

Therefore, when only tree-reducible diagrams are taken into account, the energy shift becomes exactly proportional to the density; we recover what is usually called the mean-field approximation. The method we have used is different from the method of references [11–14]; it relies on the branching properties of tree-reducible diagrams and not on the use of complex variables. Moreover, as we will see below, the method can be transposed to quantum mechanics.

Of course, equation (26) can also be obtained by the same method as these references, in a particular case: one assumes that the only non-zero irreducible cluster integral is β_1. Clearly, in this situation, all cluster integrals reduce to their tree-reducible value b_l^{R}, which can be expressed as a product of terms $b_2 = \beta_1/2$ (see Appendix A):

$$b_l^{\mathrm{R}} \equiv \frac{1}{l!} N_l \ \beta_1^{l-1} \tag{27}$$

where N_l is the number of clusters with l numbered particles and $l-1$ links, *i.e.* the number of classical tree-diagrams containing l particles:

$$N_l = \sum_{\{\text{tree diagrams}\}} \frac{(l-1)!}{\Pi_i (r_i)!} \cdot \tag{28}$$

If we insert the corresponding value of b_l into equations (2) and (3), we obtain again equation (26). Moreover, equation (17) then becomes:

$$\frac{\beta p}{\rho} = 1 - \frac{1}{2}\beta_1(T,\mathcal{V})\ \rho = 1 - b_2(T,\mathcal{V})\ \rho \tag{29}$$

which contains only a linear density correction.

3 Quantum statistical physics: Boltzmann statistics

We now leave classical statistical mechanics and reason within quantum mechanics; in a first step, we consider distinguishable particles (Boltzmann particles), postponing the discussion of the effects of quantum statistics to the next section (bosons or fermions). We first introduce our notation and then discuss the introduction of exponentials from the structure of tree diagrams.

3.1 Notation

We assume that the Hamiltonian of the system of N non-relativistic particles is:

$$H = \sum_{i=1}^{N} H_0(i) + \sum_{i<j} V_{ij} \tag{30}$$

where $H_0(i)$ is the one-particle energy (sum of its kinetic energy plus coupling to an external potential) and where the binary interaction potential V_{ij} is a function of the distance between particles i and j:

$$V_{ij} = V(|\mathbf{r}_i - \mathbf{r}_j|) = V(r_{ij}). \tag{31}$$

As in [4], we define the Ursell operators:

$$U_1(1) = \exp\left[-\beta\, H_0(1)\right] \tag{32}$$

and:

$$U_2(1,2) = \exp\left[-\beta\left[H_0(1) + H_0(2) + V_{12}\right]\right] - U_1(1)U_1(2) \tag{33}$$

and so on for higher order Ursell operators $U_3(1,2,3)$, $U_4(1,2,3,4)$, etc. All the U_l's for $l \geq 2$ have a clustering property; for instance, the diagonal matrix elements of $\langle \mathbf{r}_1, \mathbf{r}_2 \mid U_2 \mid \mathbf{r}_1, \mathbf{r}_2 \rangle$ tend towards zero when the distance $\mid \mathbf{r}_1 - \mathbf{r}_2 \mid$ becomes larger than some microscopic distance; in other words, the matrix elements of the same operator in the momentum representation are proportional to the inverse volume $1/\mathcal{V}$. One can then express the canonical partition function Z_N as a sum of products of traces of operators U_l's, each corresponding to a given diagram. Here, since we are dealing with Boltzmann particles, the number of diagrams is smaller than in [4]; exchange cycles do not occur, which is equivalent to limit them to cycles containing one particle only – in other words we exclude all those diagrams that contain horizontal lines[2]. Going to the grand canonical ensemble, one can then show that the logarithm of the corresponding partition function $Z_{\mathrm{g.c.}}$ is given by the following sum of traces:

$$\ln Z_{\mathrm{g.c.}} = \sum_{l=1}^{\infty} \frac{z^l}{l!} \mathrm{Tr}_{1,2,\ldots,l} \left\{U_l(1,2,\ldots,l)\right\} \tag{34}$$

where the factor $1/l!$ corresponds to the weight of the diagram, which arises because there are $l!$ equivalent ways to distribute l numbered particles inside the Ursell operator, as discussed in [4].

Rather than studying a thermodynamic potential, it is often more convenient to focus the discussion on the single particle density operator $\rho_I(1)$, as in reference [6]. One then gets:

$$\rho_I(1) = zU_1(1) + z^2\, \mathrm{Tr}_2\left\{U_2(1,2)\right\} + \frac{z^3}{2!}\, \mathrm{Tr}_{2,3}\left\{U_3(1,2,3)\right\} + \ldots \tag{35}$$

Now, because particle 1 is "tagged", it plays a special role, so that the generic term of this series is:

$$\frac{z^l}{(l-1)!} \mathrm{Tr}_{2,3,\ldots,l}\left\{U_l(1,2,3,\ldots,l)\right\} \tag{36}$$

with a weight $1/(l-1)!$ corresponding to the equivalent distributions of all the untagged particles. In the usual

[2] As usual, we retain the overall $1/N!$ factor in the symmetrizer, in order to avoid some well-known difficulties of classical statistical mechanics (Gibbs paradox, etc.).

graphical representation or Ursell diagrams [4,6], where vertical lines symbolize U_l operators (for $l \geq 2$) and horizontal lines exchange cycles (we have already mentioned that, since here we are dealing with distinguishable particles, no cycle of length greater than one occurs), equation (35) becomes:

$\rho_I(1) =$  (37)

At this stage, it is convenient [6,18] to express the second rank operators U_2 in terms of the operator $\overline{U}_2$ defined by:

$$U_2(1,2) = \sqrt{U_1(1)U_1(2)}\ \overline{U}_2(1,2)\ \sqrt{U_1(1)U_1(2)} \quad (38)$$

(for the moment, when $l > 2$, we do not specify the exact relation between an U_l operator and $\overline{U}_l$, but we will come back to this point later). We note that, here, $\overline{U}_2$ is defined symmetrically, with square roots of U_1 operators on each side (U_1 is a positive operator), so that $\overline{U}_2$ is Hermitian – this was not the case in [19]. The introduction of $\overline{U}_2$ has two advantages. First, factorizing the kinetic energy brings the formalism closer to classical statistical mechanics, where kinetic energy always factorizes out exactly; in other words, $\overline{U}_2(i,j)$ is the quantum equivalent of f_{ij}, although it is not strictly analogous (in quantum mechanics operators do not necessarily commute, so that the kinetic energy can still play a role in $\overline{U}_2(i,j)$). Second, in the limit of low energies, it is possible to make use of the MIME (momentum independent matrix elements) approximation, where the diagonal matrix elements of $\overline{U}_2$ are constants – see for instance the characterization of the diagonal elements of $\overline{U}_2$ in terms of the Ursell length in [19]. Graphically, in order to distinguish U_2's from $\overline{U}_2$'s in diagrams, we use two vertical parallel lines in the former case, as in [4] and [5], but only a single line for $\overline{U}_2$'s.

3.2 Tree-reducible part of $\overline{U}_l$ and U_l

For any value of l, we now define the tree-reducible operator (or fully reducible operator) $\overline{U}_l^{\mathrm{R}}$ by analogy with the tree-reducible part of a classical cluster b_l. Since the classical links correspond to $\overline{U}_2$ operators in quantum mechanics, and since the minimal number of links is $l-1$, we will express the fully reducible operator $\overline{U}_l$ as a product of $l-1$ operators $\overline{U}_2$; in addition, we also have to take into account the fact that operators do not necessarily commute with each other and apply an appropriate symmetrization. We will therefore define $\overline{U}_l^{\mathrm{R}}$ by a double sum:

$$\overline{U}_l^{\mathrm{R}}(1,2,...,l) = \sum_{\{\overline{U}_2\}} \frac{1}{(l-1)!} \times \sum_{\{\text{op. orderings}\}} \overline{U}_2(.,.)\,\overline{U}_2(.,.)\ ...\ \overline{U}_2(.,.). \quad (39)$$

The first sum symbolizes all different ways to choose sets of $l-1$ operators $\overline{U}_2$ so that the product correspond to a minimally connected cluster – in other words, in all classical tree-diagrams, we replace each f_{ij} by the corresponding $\overline{U}_2(i,j)$. The second sum, together with the factor $1/(l-1)!$, corresponds to an average of the product of all operators over all possible orderings of these $l-1$ operators. With this definition, $\overline{U}_l^R$ is obviously Hermitian as well as symmetrical with respect to all particles 1, 2,..., l. For instance:

$$\begin{aligned}\overline{U}_3^{\mathrm{R}}(1,2,3) = {} & \frac{1}{2!}[\overline{U}_2(1,2)\overline{U}_2(1,3) + \overline{U}_2(1,3)\overline{U}_2(1,2)] \\ & + \frac{1}{2!}[\overline{U}_2(1,2)\overline{U}_2(2,3) + \overline{U}_2(2,3)\overline{U}_2(1,2)] \\ & + \frac{1}{2!}[\overline{U}_2(1,3)\overline{U}_2(2,3) + \overline{U}_2(2,3)\overline{U}_2(1,3)].\end{aligned} \quad (40)$$

We now wish to define an operator U_l^{R} that we will call the tree-reducible part of U_l. The first idea that comes to mind is to mimic (38) and to define U_l^{R} by just multiplying $\overline{U}_l^{\mathrm{R}}$ on both sides by a product of $\sqrt{U_1}$'s. This is possible, but it turns out that this definition would be less convenient than another slightly different possibility, where some square root operators are inserted at different places. To introduce this definition, we first remark that each term in the first summation of (39) can be associated with a tree, exactly as in the classical tree of Figure 1, where particle 1 is put at the root, and all the rest of the diagram is built exactly in the same way (the f_{ij}'s are replaced by $\overline{U}_2(i,j)$'s). The problem now is how to properly "dress" this diagram with $\sqrt{U_1}$'s in order to build a proper U_l^{R}; we will do this operation progressively, starting from the root. For particle 1, we choose to put $\sqrt{U_1(1)}$ on each side of $\overline{U}_l^{\mathrm{R}}$, as in (38). We then progress along the branches of the tree; we first consider all $\overline{U}_2(1,j)$'s that start from the root, and associate to each of them one $\sqrt{U_1(j)}$ that is inserted directly on the right side of this $\overline{U}_2$ operator; the other $\sqrt{U_1(j)}$ is merely put at the end, after all the $\overline{U}$'s. We then proceed to apply exactly the same method to the "second generation" of $\overline{U}_2(j,k)$'s, and again insert one $\sqrt{U_1(k)}$'s directly on their right side, another at the end, etc.. We continue this operation until the whole tree is dressed with U_1's; the construction is sketched in Figure 2, which shows the association between the additional U_1's and the initial $\overline{U}_2$'s. Applying this dressing procedure to each term of the right hand side of (39) leads to an operator that we note $\widehat{U}_l^{\mathrm{R}}$. For instance, if $l = 3$, we have:

$$\begin{aligned}\widehat{U}_3^{\mathrm{R}}(1,2,3) = {} & \frac{1}{2}\sqrt{U_1(1)}\Big[\overline{U}_2(1,2)\sqrt{U_1(2)}\,\overline{U}_2(1,3)\sqrt{U_1(3)} \\ & + \overline{U}_2(1,3)\sqrt{U_1(3)}\,\overline{U}_2(1,2)\sqrt{U_1(2)} \\ & + \overline{U}_2(1,2)\sqrt{U_1(2)}\,\overline{U}_2(2,3)\sqrt{U_1(3)} + ...\Big] \\ & \times\sqrt{U_1(1)U_1(2)U_1(3)}.\end{aligned} \quad (41)$$

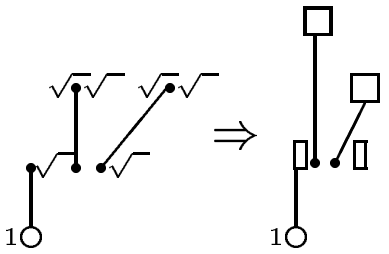

Fig. 2. In this diagram, the single lines symbolize $\overline{U}_2$ operators (as opposed to double lines which symbolize U_2's in Ursell diagrams). The figure illustrates symbolically how $\sqrt{U_1}$'s (symbolized as squareroots $\sqrt{\ }$ in the left part, as rectangles in the right part) are inserted into each product of $\overline{U}_2$'s that appears in $\overline{U}_l^{\mathrm{R}}$, in order to build an operator U_l^{R}.

Finally, to make sure that the operator U_l^{R} is Hermitian, we simply define it as the Hermitian part of $\widehat{U}_l^{\mathrm{R}}$:

$$U_l^{\mathrm{R}}(1,2,...,l) = \frac{1}{2}\left[\widehat{U}_l^{\mathrm{R}}(1,2,...,l) + \left(\widehat{U}_l^{\mathrm{R}}(1,2,...,l)\right)^{\dagger}\right] \tag{42}$$

(we will nevertheless see that, in practice, this symmetrization has no consequence on the following calculations, which deal only with partial traces: the distinction between $\widehat{U}_l^{\mathrm{R}}$ and U_l^{R} is not essential here).

3.3 Partial trace

We now study the following partial trace with respect to particles 2, 3, ..., l:

$$\mathrm{Tr}_{2,3,...l}\left\{U_l^{\mathrm{R}}(1,2,3,...,l)\right\} \tag{43}$$

which is still an operator in the space of states of particle 1. Since U_l^{R} is obtained from (39) by adding $\sqrt{U_1}$'s at appropriate places in each term of the sum, the trace contained in (43) can itself be expressed as a sum of traces of products of operators. To each of these terms, we will now associate another sort of tree diagram, which resembles that of Figure 2, but where the order of the branches now characterize the order of operators under the trace (instead of being related to the numbering of the particles).

3.3.1 Normal ordering

The purpose of this section is to put the operators in a standard order that can be described by a tree-diagram corresponding to a well-defined contribution to the value of the partial trace that provides ρ_1. As before, the open circle at the root of the tree corresponds to particle 1, but now the upper branch corresponds to the first sequence of operators that occur inside the trace, the first sub-branch to the second sequence, etc. This new tree is actually not very different from the initial tree: the only difference is actually the way in which the ordering of its branches is defined.

Let us first consider a given term contained in the right hand side of (39), and suppose that we are interested in its partial trace – for the moment we leave aside the $\sqrt{U_1}$'s, and define the notion of "normal ordering" for the partial trace of any term that appear in the sum defining $\overline{U}_l(1,2,...l)$. To reach this normal ordering, the first step is to locate the first operator of the product that contains particle 1, as well as some other particle i, $\overline{U}_2(1,i)$, and to move it to the front (the left side of the product): all operators that occurred before are moved to the end of the series (the right), in the same order, by using the property of circular permutation under the trace. The second step is to locate, among all operators now sitting after this operator, which is the first operator $\overline{U}_2(i,j)$ containing i, and to move it to the second position, directly to the right of $\overline{U}_2(1,i)$; this is possible since, if the intermediate operators do not contain[3] particle 1, they can be moved to the left of $\overline{U}_2(1,i)$ and then to the end of the series; if they contain particle 1, they cannot contain[4] particle j, so that they can be moved just after $\overline{U}_2(i,j)$. The series now begins with the product $\overline{U}_2(1,i)\overline{U}_2(i,j)$. The third step is similar to the second: one locates on the right of $\overline{U}_2(i,j)$ the first operator that contains particle j, $\overline{U}_2(j,k)$, and moves it directly to the third rank, by the same method: if the intermediate operators contain[5] neither particle 1 nor particle i, nor particle j, they are moved to the front and then to the end; if they contain one of them, they do not contain[6] particle k, they are moved just after $\overline{U}_2(j,k)$. The series now begins with the product $\overline{U}_2(1,i)\overline{U}_2(i,j)\overline{U}_2(j,k)$. The same process continues by iteration until, at some point, one reaches the end of the branch of the tree, with a numbered particle that does not occur any other $\overline{U}_2$.

One then proceeds to construct a new branch, and therefore to select a ramification point. For this purpose, one goes backwards from the end along the first branch, locates the first numbered particle m, in operator $\overline{U}_2(m,p)$, that occurs (at least) a second time in the list of remaining operators, in $\overline{U}_2(m,n)$; this latter operator is then moved directly to the right of $\overline{U}_2(m,p)$, and creates the starting point of another branch. The new branch is then extended by the same method as the first. When this branch is also finished, two cases may occur: either particle m occurs a third time (or more), so that three branches (or more) of the tree will originate from the same point; or particle m does not occur anymore, and one continues to move backwards in the main branch to find another particle that occurs again in one of the non-ordered $\overline{U}_2$'s. At some point,

[3] They cannot contain particle i by assumption.

[4] They cannot contain both particles 1 and j, since otherwise the two particles would be linked twice, which is contradictory with the tree structure of Figure 2.

[5] They cannot contain particle j by assumption.

[6] The intermediate operators can not contain at the same time particle k and either particle 1, or i or j: for instance, if they contained k and i, those two particles would be linked twice (directly and through particle j), which is contradictory with the structure of the tree-diagram.

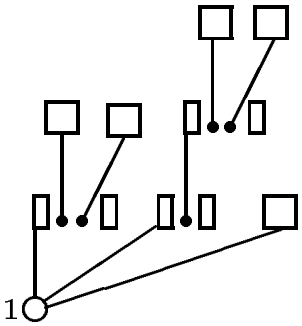

Fig. 3. This figure shows a ρ_1 tree-diagram where the order of the branches now determines the order of operators inside a trace over variables of all particles, except particle number 1; the first vertical branch corresponds to the first group of operators, the first secondary branch on the right to the next group, etc. Moreover, each $\overline{U}_2$ carries with it two $\sqrt{U_1}$ operators; in order to simplify the diagrams, we represent them as half-squares (rectangles). A full square represents a U_1 operator.

all operators have been moved to their appropriate place, and the process stops.

Now, to get the contribution to the trace, we have to add $\sqrt{U_1}$'s at the appropriate places, but this does not change much to the reasoning that me have made for reaching the normal ordering of the operators: the $\sqrt{U_1}$'s at the end of the product do not move during the operation, while those that directly follow $\overline{U}_2$'s move together with this operator (this is possible since they do not change the commutations rules). Consequently, all operators can be put into their normal ordering exactly in the same way, as for $\overline{U}_2$'s only.

Obviously, the numbering of all particles, except particle 1, is totally irrelevant for the value of the trace, since it defines dummy variables; what is important is the geometry of the tree, since it determines the value of the operator obtained after the partial trace is taken[7]. Therefore, a diagram such as that of Figure 3 corresponds to a well-defined contribution to the trace. Another remark is that the contribution of $\widehat{U}_l^{\mathrm{R}}$ to the trace already provides an Hermitian operator acting on particle 1: by circular permutation under the traces, it is easy to see that the only change induced by a reversing of the order of the operators leads to a thee where the order of the branches is reversed, in other words to a tree that already exists in $\widehat{U}_l^{\mathrm{R}}$ and ensures Hermiticity of the partial trace. This means that the Hermitian symmetrization of (42) is actually not necessary; from now on, we will therefore only consider the trace of $\widehat{U}_l^{\mathrm{R}}$.

3.3.2 Weights of tree-diagrams

From the results of the preceding section, we can express the partial trace of $\widehat{U}_l^{\mathrm{R}}$ as a sum over all diagrams such as that of Figure 3; we now wish to know what their weight is, or in other words, how many terms of the double sum (39) correspond to each diagram. The reasoning is analogous to the reasoning of Section 2.3, except that now we are dealing with order of operators, instead of particle numberings. Suppose that we ascribe arbitrary particle numbers to all nodes of this diagram – since particle 1 is always at the root of the diagram, this can be done in $(l-1)!$ different ways. To each of these numberings corresponds a given sequence of $\overline{U}_2$ operators, and therefore a given term of the first summation of (39). Now, how many terms of the second summation then correspond to this given diagram? To answer this question depends on the branching (or ramification) factors r_1, r_2, etc. defined in Section 2.3. In the list of $\overline{U}_2$'s, the only non-commuting operators are those which contain one common particle[8]. Starting from any order of operators, and after ordering them according to the procedure of Section 3.3.1, it is easy to see that there is a probability $1/(r_1)!$ that the first ramification will take place with the appropriate order of chain of operators, a probability $1/(r_1)!(r_2)!$ that the right order is still obtained after two ramifications, etc. Finally, among all operators that are contained in the second sum of (39), the number or terms that correspond to each tree-diagram is:

$$\frac{(l-1)!}{\Pi_i(r_i)!}\,. \tag{44}$$

If we take into account the factor $(l-1)!$ mentioned before (corresponding to the first summation) as well as the factor $1/(l-1)!$ which is explicit in (39), we obtain the following weight of the tree-diagram:

$$(l-1)!\frac{1}{(l-1)!}\frac{(l-1)!}{\Pi_i(r_i)!} = \frac{(l-1)!}{\Pi_i(r_i)!} \tag{45}$$

so that we eventually obtain:

$$\mathrm{Tr}_{2,3,\ldots l}\left\{U_l^{\mathrm{R}}(1,2,3,...,l)\right\} = \sum_{\{\rho_1 \text{ diagrams}\}} \frac{(l-1)!}{\Pi_i(r_i)!}\, T_{\mathrm{diag.}}(1) \tag{46}$$

where $T_{\mathrm{diag.}}(1)$ is the operator (acting on the variables of particle 1) that is obtained by the partial trace corresponding to the diagram with branching factors r_1, r_2, etc.

3.4 Energy shift for ρ_{I}

The next step is to obtain the one-particle density from the previous considerations. Its expression in terms of Ursell operators [5] (only retaining their tree-reducible part) is:

$$\begin{aligned}\rho_I(1) = {} & zU_1(1) + z^{\,2}\mathrm{Tr}_2\left\{U_2^{\mathrm{R}}(1,2)\right\} \\ & + \frac{z^3}{2!}\,\mathrm{Tr}_{2,3}\left\{U_3^{\mathrm{R}}(1,2,3)\right\} + ... \\ & + \frac{z^{l-1}}{(l-1)!}\,\mathrm{Tr}_{2,..,l}\left\{U_l^{\mathrm{R}}(1,...,l)\right\} + ...) + ...\end{aligned} \tag{47}$$

[7] But different trees do not necessarily correspond to different results.

[8] They never contain two, otherwise the diagram would not be minimally connected.

Replacing the reduced Ursell operators by their expression as sums of tree-diagrams and taking the counting factors into account (45), we see that ρ_I becomes:

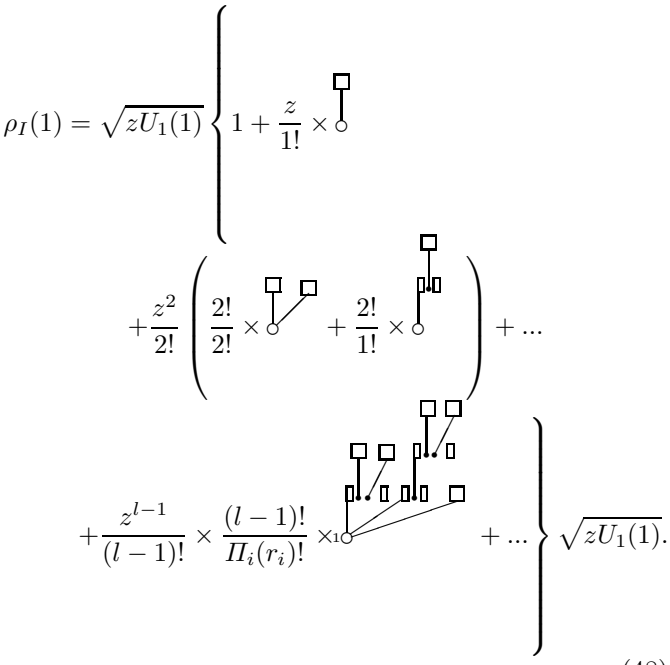

(48)

It is now possible to regroup diagrams according to the "first branching factor" $1/(r_1)!$, and to write:

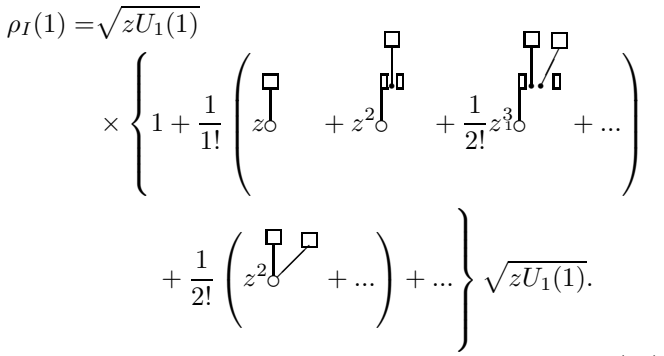

(49)

Again, we notice a self-similarity property of the expansion, which makes one-particle density operators appear on the right hand side of the equation:

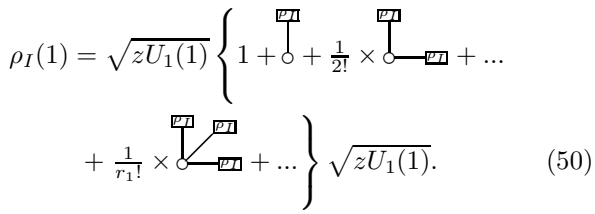

(50)

We now recognize the development of an exponential operator, and finally obtain:

$$\rho_I(1) = \sqrt{zU_1(1)}\exp\left(\mathrm{Tr}_2\left\{\overline{U}_2(1,2)\,\rho_I(2)\right\}\right)\sqrt{zU_1(1)} \tag{51}$$

or:

$$-\beta\Delta(1) = \mathrm{Tr}_2\left\{\overline{U}_2(1,2)\,\rho_I(2)\right\}\cdot \tag{52}$$

We therefore find that the energy shift depends linearly on the one-particle density operator (proportional to the density), which corresponds exactly to the mean-field approximation.

3.5 Physical discussion

The preceding calculation illustrates the physics that is behind the construction of a mean-field: when the test particle 1 interacts with another particle i, it is also possible that this particle interacts in turn with particle j, and so on. Moreover, either the test particle or any other particle may perfectly well interact with several others; this introduces branching in the interaction tree, either directly at the root or at any other place. What is not possible is to create "loops": any particle can interact with one or several neighbors, and these interactions can propagate further to other particles through many intermediate carriers, but they should never come back to the original particle. This is very similar to the "no re-collision" assumption which is behind the "molecular chaos Ansatz" of the Boltzmann transport equation.

We note that the expression (52) involves the operator $\overline{U}_2(1,2)$, instead of the potential itself V_{12} as in the usual expressions of the mean-field. In other words, the mean-field involves matrix elements of an exponential containing the interaction potential (see definition (33) of the second Ursell operator), more precisely the difference between two exponentials (corresponding to a change of the local Boltzmann equilibrium), instead of not merely the matrix elements of V_{12} itself. Of course, if this potential can be treated to first order, this makes no difference, as shown by an elementary calculation. But realistic interatomic potentials can not be treated properly by first order perturbation theory (Born approximation), and this exponential may actually introduce an enormous difference. A well-known illustration of this fact is given by alkali atoms, which have a strongly attractive potential sustaining many bound states (V_{12} is negative, except in the very short range part of the potential); nevertheless, the phase shift at zero energy may correspond, either to a positive scattering length (effective repulsion), or to a negative value (effective attraction), depending on small details of the potential and on a very delicate balance effect between attraction and repulsion[9]. A naive reasoning in terms of the potential itself could lead to the idea that, in a dilute gas of alkali atoms, the mean-field should always be very attractive. Of course, this is known to be incorrect: the mean-field is actually repulsive when a is positive, and attractive only when a is negative. The usual

[9] Even a purely attractive potential may have a positive or negative scattering length, depending on the position of the last bound state with respect to the continuum.

way to understand this property is to replace the real potential V_{12} by a pseudo-potential, which is directly proportional to the scattering length a and treated to first order, a somewhat heuristic method (since the exact reason why using the real potential is incorrect is not so clear). Here, we clearly see that what appears naturally is the matrix elements of $\overline{U}_2(1,2)$; as shown in [19], the latter can be expressed in terms of phase shifts and be shown to be proportional to the scattering length[10] a: for instance, if the latter is positive, we directly get a positive value for the mean-field, without any special manipulation[11].

Another remark is that (51) and (52) give ρ_I as the product of exponentials, and not the exponential of a sum, which is not the same thing if the operators do not commute. For translationally invariant systems, this distinction vanishes since all the single particle operators are diagonal in the same basis (the momentum basis), and therefore commute. In other cases, one should be careful to take into account non-commutativity of operators; for instance, the Hermitian operator Δ can not be seen exactly as a correction to the one-particle Hamiltonian.

Finally, we remark that our reasoning could be generalized. Here, we have expressed all reducible parts of Ursell operators in terms of $\overline{U}_2$, which is its own irreducible part; we have left aside the irreducible part $\overline{U}_3^{\text{Irr.}}$ of $\overline{U}_3$. But it should be possible to go further, and to use $\overline{U}_3^{\text{Irr.}}$ as the starting point of another decomposition of all $\overline{U}_l$'s for $l \geq 4$; in this way, all these $\overline{U}_l$'s could give a contribution to the energy shift Δ that is quadratic in the density. More details on this calculation are given in Appendix C.

4 Quantum statistical physics: identical particles

The formalism for identical (Bose or Fermi) particles differs from Boltzmann particles by the inclusion of exchange cycles. They introduce horizontal parts in the Ursell operator diagrams [4–6], which combine with the vertical lines associated with the Ursell operators; many more diagrams have to be taken into account in order to include quantum statistics. Despite this big difference, we will see that the formalism introduces almost the same mechanism and that the exponential of energy corrections also appear naturally.

[10] More precisely, this is true for the dominant part of the matrix element, which depends on the value of the collision wave functions outside of the interaction potential (asymptotic value of the scattering states). Another contribution arises from the wave functions inside the potential. Nevertheless, if the range of the potential is very small, the latter contribution remains negligible.

[11] Of course, other methods to prove the same result also exist; for instance, in the Green's function formalism, the summation of an infinite series of ladder diagrams can be used to construct the scattering length from the potential itself.

4.1 General equations

As shown in reference [5], for identical particles, equation (35) should be replaced by:

$\rho_I = f_1 +$ 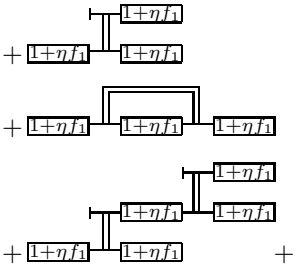 (53)

where f_1 is the one-particle density operator for an ideal gas:

$$f_1(1) = \frac{zU_1(1)}{1 - \eta\, zU_1(1)} \tag{54}$$

with $\eta = +1$ for bosons, $\eta = -1$ for fermions. In (53), the operators $[1 + \eta f_1]$ arise from a summation over all possible values of cycle length l (ranging from $l = 0$ to infinity) of the product $[\eta z U_1(1)]^l$ - the origin of the factor η is that, for fermions, every exchange cycle of length l introduces a $(-1)^l$ sign into the diagram which contains it. Generally speaking, in all such diagrams, the lowest horizontal line corresponds to the multiplication of operators acting in the space of particle 1, while all the other lines above correspond to traced variables of other particles.

In [6], the series giving ρ_I was re-written in a self-consistent way, which resums in one single diagram an infinite number of diagrams of the initial series (53):

$\rho_I = f_1 +$ 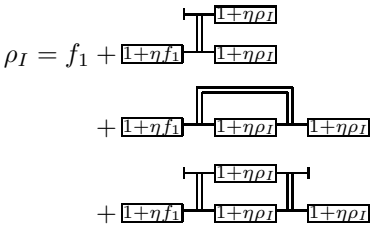 (55)

For instance, the diagram of the third line of (53), as well as many other similar diagrams, are now included in the first term after f_1 in (55), which symbolizes the partial trace:

$$2z^2\,(1+\eta f_1(1))\ \mathrm{Tr}_2\left\{U_2(1,2)\,[1+\eta\rho_I(2)]\right\}\ (1+\eta\rho_I(1))\,. \tag{56}$$

In (55), the second term after f_1 turns out to be the exchange term of (56), since it can be written:

$$2z^2\,(1+\eta f_1(1))\ \mathrm{Tr}_2\left\{U_2(1,2)\,\eta\,P_{\text{ex.}}(1,2)\ [1+\eta\rho_I(2)]\right\} \times (1+\eta\rho_I(1)) \tag{57}$$

where $P_{\text{ex.}}$ is the exchange operator between particles 1 and 2. These two terms therefore group naturally together

with the introduction of the symmetrized (S: $\eta = 1$) or antisymmetrized (A: $\eta = -1$) form of the U_2 operator:

$$U_2^{S,A}(1,2) = \frac{1+\eta P_{\text{ex.}}(1,2)}{2}\, U_2(1,2). \tag{58}$$

For a *dilute* gas, they were interpreted in [6] as the mean-field correction, which provides no correction to the critical temperature of the gas within the MIME approximation (see Sect. 3.1). The explicit expression of the third term is, similarly:

$$2z^2\,(1+\eta f_1(1))\ \mathrm{Tr}_2\,\{U_2(1,2)\ (1+\eta\rho_I(1))\ (1+\eta\rho_I(2)) \times U_2(1,2)\ (1+\eta\rho_I(2))\ (1+\eta\rho_I(1))\} \tag{59}$$

and, as the preceding term, it groups with another diagram (not shown) that appears as its exchange diagram.

4.2 Introducing exponentials

Our purpose now is to introduce exponentials in order to make energy shifts appear explicitly. For the ideal gas, the one particle distribution is given by (54) so that, since $\eta^2 = 1$:

$$1+\eta\,(f_1)^{-1} = \eta\ \ [zU_1]^{-1} = \eta \exp\left[\beta\,(H_1(1)-\mu)\right]. \tag{60}$$

Similarly:

$$\eta\ \left[1+\eta\,(f_1)^{-1}\right]^{-1} = \frac{f_1}{1+\eta f_1} = z\,U_1 \tag{61}$$

where the same exponential appears, now with a negative exponent. To calculate energy shifts, it is therefore natural to introduce quantities such as $1+\eta(\rho_1)^{-1}$ or $\rho_1/(1+\eta\rho_1)$.

To do this, we remark that the lower lines of all diagrams contained in (53) start and end with the same operators, so that equation (55) can be re-written as:

$$\rho_I(1) = f_1(1) + [1+\eta f_1(1)]\ \ K(1)\ \ [1+\eta\rho_I(1)] \tag{62}$$

where the operator K is an infinite sum of partial traces, containing various number of traced U_2's as well as $[1+\eta\rho_I]$'s in the horizontal lines:

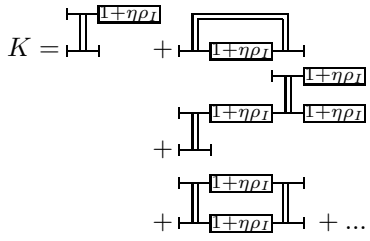

(63)

In other words, the diagrams corresponding to K are obtained from those corresponding to ρ_I by simply removing the two external parts of the lowest line (diagram amputation). The operator K is clearly Hermitian, as can be shown by using circular permutation of operators under the trace. There is an obvious analogy between operator K and the self-energies in the formalism of Green's functions.

Now, if we multiply both sides of (62) by $(f_1)^{-1}$ on the left, and by $(\rho_I)^{-1}$ on the right, we obtain:

$$(f_1)^{-1} = (\rho_I)^{-1} + \left(1+\eta\ (f_1)^{-1}\right)\ K\ \left(1+\eta\ (\rho_I)^{-1}\right) \tag{64}$$

or, if we multiply both sides by η, add 1, and take (61) into account:

$$1+\eta\ (f_1)^{-1} = \left[1+(zU_1)^{-1}\,K\right]\left[1+\eta\,(\rho_I)^{-1}\right] \tag{65}$$

or again:

$$\frac{\rho_I}{1+\eta\rho_I} = z\,U_1 + K. \tag{66}$$

In the absence of interaction, K vanishes and we recover (61); K appears therefore as analogous to a correction to zU_1 introduced by the interactions, in other words to a correction to the single particle energy.

To make this analogy more precise, by similarity with (60), we define the energy shift operator $\Delta(1)$ by[12]:

$$1+(\eta\rho_I)^{-1} = \eta\ [zU_1(1)]^{-1/2}\ \mathrm{e}^{\beta\Delta(1)}\ [zU_1(1)]^{-1/2} \tag{67}$$

which immediately leads to:

$$\exp\{-\beta\,\Delta(1)\} = \left[1+\frac{1}{\sqrt{zU_1(1)}}\ K\,(1)\,\frac{1}{\sqrt{zU_1(1)}}\right]. \tag{68}$$

The series defining the operator $K(1)$ therefore contains all the information on the energy shifts for the single-particle density operator; equation (68) is the equivalent of relation (86) of Appendix B, in an operator form, when quantum statistics is added.

4.3 Calculating the energy shifts

Our purpose now is to express the energy shift as a function of the density, or of the single particle density operator ρ_I, as we did in classical statistical physics. This raises two problems: first, we have to build an exponential from the infinite series that provides K; second, we have to understand how the density operator ρ_I appears, instead of the factors $[1+\eta\rho_I(i)]$ that seem to be systematically present in all terms of the series. We will see that the two problems "cure each other" and that the result the calculation leads to an systematic and satisfactory grouping of the terms for a dense system. To do this, we begin with a simple case, where only the direct term of the mean-field is taken into account.

[12] We could also have used another definition of the energy shift operator, by introducing the exponential of a sum instead of the product of exponentials:

$$\left[1+(\eta\rho_I)^{-1}\right] = \eta\ \mathrm{e}^{\beta(H_1(1)+\Delta(1)-\mu)}.$$

It turns out that, for the present calculation, definition (67) is more convenient.

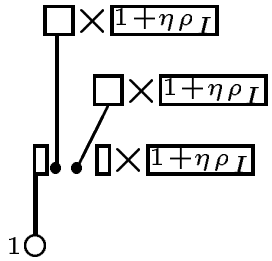

Fig. 4. With quantum statistics, this diagram replaces the diagram in the right part of Figure 2; note the presence of the statistical $[1 + \eta\rho_I]$ factors.

4.3.1 Direct term

We now take an approximation of expression (63) of K by retaining only the diagrams that contain one single U_2, one single U_3, ... one single U_l, ... and where all the U_l operators are connected to l different cycles:

$K =$ 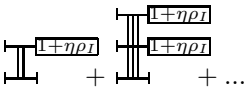 $+$ $+ \ldots$ (69)

Moreover, we replace each Ursell operators U_l by its tree-reducible part. This leads to the equation:

$$\begin{aligned} K(1) = {} & z^2\ \mathrm{Tr}_2\left\{U_2(1,2)\ [1+\eta\rho_I(2)]\right\} \\ & + \frac{z^3}{2!}\ \mathrm{Tr}_{2,3}\left\{U_3^{\mathrm{R}}(1,2,3)\left([1+\eta\rho_I(2)]\ [1+\eta\rho_I(3)]\right\}\right. \\ & + ... \\ & + \frac{z^l}{(l-1)!}\ \mathrm{Tr}_{2,..,l}\left\{U_l^{\mathrm{R}}(1,..,l)\ [1+\eta\rho_I(2)]\ldots\right. \\ & \left.\times\,[1+\eta\rho_I(l)]\right\} + ... \end{aligned} \tag{70}$$

For the sake of simplicity, we will even replace here the operators U_l^{R} by their non-symmetrized part $\widehat{U}_l^{\mathrm{R}}$ (see Eq. (42)); nevertheless, since at the end we will find an Hermitian operator, this has no consequence on the result. Graphically, if we represent as before the $\sqrt{U_1}$'s by vertical rectangles, U_1's by squares and multiplication by $[1 + \eta\rho_1]$ by long horizontal rectangles as in Figure 4, (70) then corresponds to:

$K(1) =$  $+$ 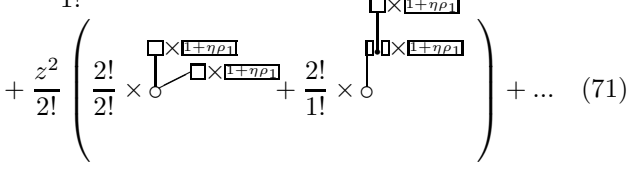 $+ \ldots$ (71)

We now notice the same kind of self-similarity of the series than in the case of Boltzmann statistics. There are nevertheless two differences. The first is that the operator that is resummed in the branches is now K, or actually the sum $zU_1 + K$ (the term zU_1 is introduced by the 1 that is present at each node but absent as the first term in the series); the second is that this operator is multiplied on the right by the factor $[1 + \eta\,\rho_I]$, so that we get the product:

$$[zU_1 + K] \times\ [1 + \eta\,\rho_I]\,. \tag{72}$$

But, according to (66), this product is merely equal to ρ_I. We therefore have:

$$K(1) = \sqrt{U_1(1)}\left[\exp\left(\mathrm{Tr}_2\left\{\overline{U}_2(1,2)\,\rho_I(2)\right\}\right) - 1\right]\sqrt{U_1(1)} \tag{73}$$

(the -1 arises because the first term of the exponential series is absent from K). Inserting this result into (68) finally provides:

$$-\beta\Delta(1) = \mathrm{Tr}_2\left\{\overline{U}_2(1,2)\rho_I(2)\right\} \tag{74}$$

which is exactly the same result as for Boltzmann statistics. We can now check that the final result is Hermitian, so that it was indeed correct to ignore the Hermitian symmetrization of the operators $\widehat{U}_l^{\mathrm{R}}$.

4.3.2 Exchange term

We now add exchange terms into (69). An example of such a term is the second term of the right hand side of (63): we have already noticed that this term is obtained by replacing $\overline{U}_2(1,2)$ by $\overline{U}_2(1,2)P_{\mathrm{ex}}$ in the direct mean-field term associated with the linear density term in K. In other words, the sum of the two terms corresponds to the following substitution:

$$\overline{U}_2(1,2)\ \Rightarrow\ \overline{U}_2(1,2)\ [1 + \eta P_{\mathrm{ex.}}(1,2)] = 2\,\overline{U}_2^{S,A}(1,2) \tag{75}$$

where $P_{\mathrm{ex.}}(1,2)$ is the exchange operator for particles 1 and 2. More generally, the question is whether each term in the whole series of terms of (71), which eventually leads to an exponential, contains all exchange terms that are necessary to perform substitution (75).

In order to construct the diagrams which are exchange diagrams for the mean-field, it is useful to remember the origin of each Ursell diagram: it arises from the association of a set of U_l's (with $l \geq 2$) with permutation cycles; in the diagrams that we have retained so far, only one U_l is present, and each of the l particles is included in a different cycle, containing none of the other particles. Let us now consider two particles, i and k, that sit initially in different cycles; if we apply an additional exchange operator $P_{\mathrm{ex}}(i,j)$ to the product of the two cycles, it is easy to see that we obtain a larger cycle with an length which is the sum of the two initial lengths: the two cycles merely coalesce into one. This immediately leads to another Ursell diagram, such as the two first that are shown in Figure 5 (a and b) in the particular case $l = 3$. One can then repeat the operation and apply another exchange operator to the result, which will make two more cycles fuse together into

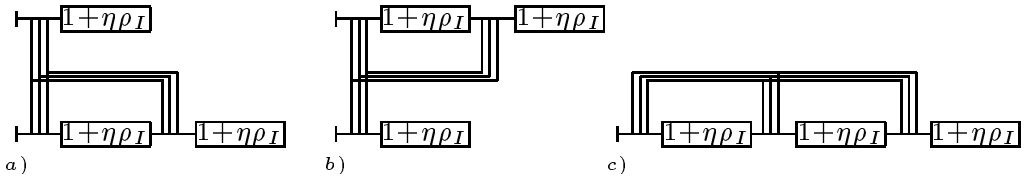

Fig. 5. Exchange diagrams for the case $l = 3$; the direct term from which these diagrams are obtained is the second term in the right hand side of (69).

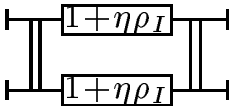

Fig. 6. An example of a "correlation diagram", where exchange cycles and Ursell operators (U_2's *e.g.*) combine to make a "loop". This diagram provides a contribution which is beyond mean-field.

an even larger cycle; in this way still another diagram is obtained, such as the last shown in Figure 5c. This introduction of exchange may be repeated until all pairs of particles contained in $\overline{U}_2$ links are exchanged, which leads to a maximum cycle of length l containing all of them. Altogether, $2^{l-1} - 1$ different diagrams correspond to all possible ways to fuse together the various cycles; they provide all the exchange diagrams associated with the initial direct diagram.

Finally, we have to replace in all these diagrams U_l by the sum of product of $\overline{U}_2$ operators that corresponds to U_l^{R}, as we did for the direct terms; we replace the "skeleton" provided by U_l by all possible trees. The result of this operation is the same as for the direct terms: any branching at the root introduce a product of operators, while branching at the other nodes introduces a product inside a partial trace. The situation is thus not different than before, except that two sorts of links now occur, with or without exchange; the summation of the series then provides nothing but the exponential of a sum. We therefore obtain the simple result:

$$-\beta\Delta(1) = \mathrm{Tr}_2 \left\{ \overline{U}_2(1,2) \left[1 + \eta P_{\mathrm{ex.}}(1,2) \right] \rho_I(2) \right\} \qquad (76)$$

which shows that it is the symmetrized form of $\overline{U}_2$ that appears naturally in the expression of the mean-field.

4.3.3 Correlations

Can we go further in this exponentiation, and try to include in the energy shift terms such as that corresponding to the diagram of Figure 6?

As we have seen, the exponentiation operation involves the consideration of operators that are the square, the cube, etc. of the lowest order operator. Could we somehow consider diagrams such as that of Figure 6, but where U_3 are introduced, replace U_3 by a tree diagram, and show that the result is the square of the initial operator? Actually, this does not seem to be possible. One reason is that the square of an operator such as that shown in Figure 6 would involve particle 1 to be part of two independent cycles, a situation that never occurs in Ursell diagrams. For this reason, we have not been able to exponentiate the diagram of Figure 6. One possibility is to consider this class of terms as small correction to the mean-field exponential terms, to be treated linearly (as was done for instance in [6]). This is indeed possible above the Bose-Einstein transition point, but it is certainly not correct below this point, as we discuss below. As a consequence, the validity of our calculations is limited to non-condensed Bose systems.

4.4 Physical discussion

The energy shift operator $\Delta(1)$ is reminiscent of the self-energy operator of temperature Green's function's theories, but actually it corresponds to a different notion. Self-energies include a notion of time, or frequency (or Matsubara discrete frequencies), while time evolution is absent from the formalism of Ursell operators: only equilibrium properties are obtained, which excludes notions such as time dependent response functions, collective modes and quasiparticles. In other words, only the equilibrium single particle density operator is calculated, which contains less information (integrated information over all frequencies) than full Green's functions. It is nevertheless interesting to see how the formalism manages to reconstruct the energy exponentials, with or without exchange cycles, and that at the end the mean-field expression simplifies to introduce the single particle density operator itself in a consistent way. It is also worth noticing that the relevant matrix elements to calculate this mean field are not those of the bare interaction potential V_{12}, but rather those of an operator $\overline{U}_2(1,2)$ that contains V_{12} in an exponential - we have already discussed in Section 3.5, its relation with the introduction of the scattering length as the relevant parameter to describe the interactions.

Of course, one should keep in mind that the notion of mean-field is not exact: we have summed only limited classes of diagrams; moreover, we have replaced the U_l's by their reducible part U_l^{R}. In the case of bosons for instance, it is known [6,20] that correlation diagrams such as that shown in Figure 6 play an essential role just above the Bose-Einstein transition point, and even that the theory takes a non-perturbative character at the transition temperature, so that no limitation to any finite set of diagrams (or of class of diagrams) is in principle possible. Below the condensation point, the situation is even more

dramatic. The reason is that a ladder diagram with M ladders (U_2 operators) and an intermediate state with an extensive population (the condensed state) is proportional to the $\mathcal{V}^{M-2}$ (where $\mathcal{V}$ is the volume), which makes it diverge in the thermodynamic limit as soon as $M \geq 3$: however small the interaction parameter is, these terms will always dominate the others in the thermodynamic limit. A similar situation occurs for the so called "bubble diagrams". As a consequence, since we have ignored all these correlation diagrams, in their present form our calculations have a validity that is limited to non-condensed boson systems. Actually, one would expect that, in a condensed system, the mean-field should include two different parts, due to excitations and to the condensate respectively, but for the moment we have not explored this question.

5 Conclusion

At the end of their 1938 article, Kahn and Uhlenbeck [21] remark that "[they] have not been able to generalize this physical interpretation of the β_l [(irreducible cluster integrals)] to the quantum theory." In the present article, we have achieved this goal: we have provided a consistent derivation of the exponentials that introduce the energy shifts Δ, from which the equation of state can in turn be derived as in classical statistical physics. Actually, in the article, we emphasize how the linear density term can be derived, but Appendix C discusses briefly how higher order density terms could also be included. For a classical system, our method is different, and in a sense simpler, than that of Hansen and McDonald [10]; it does not require any reasoning in the complex plane and we have shown how the exponentials of ρ_I appear rather naturally in the calculations. The operator that plays the basic role in all our calculations is $\overline{U}_2(1,2)$; its matrix elements depend on the asymptotic (long distance) properties of the two body scattering wave functions. But, in fact, $\overline{U}_2(1,2)$ contains more information than only asymptotic wave functions and phase shifts: it also contains information about short range effects of the potential (atoms in the middle of a collision) as well as about bound states; it would be interesting to explore their consequences on the properties of the mean-field.

Appendix A

In this appendix, we explain why classical tree-diagrams consisting of l particles all have the same numerical value, namely $(\beta_1)^{l-1}$. Let us consider the following integral corresponding to a l particles tree-diagram:

$$T_{\text{diag.}} = \frac{1}{\mathcal{V}} \int \mathrm{d}^3 r_1 \, \mathrm{d}^3 r_2 ... \mathrm{d}^3 r_l \; f_{12} ... f_{ij} ... f_{kl}. \tag{77}$$

Each Mayer function appearing in it depends on the relative distance between two particles:

$$f_{ij} = f(|\mathbf{r}_i - \mathbf{r}_j|) = f(r_{ij}). \tag{78}$$

Let $\mathbf{x}_k$ be the relative position vector between particle k and the preceding particle in the branch starting from the root. There is $l-1$ such vectors ($k = 2$ to l). The important thing to notice is that each Mayer function depends on only one $\mathbf{x}_k$, and that two Mayer functions in the product necessarily depend on different $\mathbf{x}_k$. Let

$$\mathbf{R} = \frac{1}{l} \left(\mathbf{r}_1 + \mathbf{r}_2 + ... + \mathbf{r}_l \right) \tag{79}$$

be the center of "mass" position vector. Then making a change of variables in the integral from ($\mathbf{r}_1$, $\mathbf{r}_2$,..., $\mathbf{r}_l$) to ($\mathbf{R}$, $\mathbf{x}_2$,..., $\mathbf{x}_l$) (the Jacobian is one), we obtain:

$$T_{\text{diag.}} = \frac{1}{\mathcal{V}} \int \mathrm{d}^3 R \; \mathrm{d}^3 x_2 ... \mathrm{d}^3 x_l \; f(x_2) \; ... f(x_l). \tag{80}$$

We can then integrate over the variable $\mathbf{R}$ to get rid of the volume factor. The $l-1$ integrals that are left separate so that:

$$T_{\text{diag.}} = \int \mathrm{d}^3 x_2 \; f(x_2) ... \int \mathrm{d}^3 x_l \; f(x_l) = \left(\int \mathrm{d}^3 x \; f(x) \right)^{l-1}. \tag{81}$$

But the integral of the Mayer function is precisely what we called the first irreducible cluster integral β_1 (see Eq. (15)), so that we finally get:

$$T_{\text{diag.}} = (\beta_1)^{l-1}. \tag{82}$$

Appendix B

In this appendix, we emphasize the similarity between the equation that gives the energy shift as a function of the density and the elimination of z between (2) and (3) that provides the equation of state. For simplicity, we assume that no external potential acts on the particles, so that translational invariance is satisfied. We call ρ_k the diagonal elements of ρ_I:

$$\rho_{\mathbf{k}} = \langle \mathbf{k} \mid \rho_I \mid \mathbf{k} \rangle \tag{83}$$

and $u_1(\mathbf{k})$ those of U_1:

$$u_1(\mathbf{k}) = \langle \mathbf{k} \mid U_1 \mid \mathbf{k} \rangle = \mathrm{e}^{-\beta e_k}$$

where e_k is the single particle kinetic energy. As for the diagonal elements of U_2 in the momentum representation, we note them:

$$u_2(\mathbf{k}_1, \mathbf{k}_2) = \langle \mathbf{k}_1, \mathbf{k}_2 \mid U_2 \mid \mathbf{k}_1, \mathbf{k}_2 \rangle$$

(for the moment we do not make the MIME approximation), $u_3(\mathbf{k}_1, \mathbf{k}_2, \mathbf{k}_3)$ for those of U_3, etc. Equation (35) then provides:

$$\rho_{\mathbf{k}} = u_1(\mathbf{k}) \left[z + z^2 \sum_{\mathbf{k}'} u_2(\mathbf{k}_1, \mathbf{k}_2) \, u_1(\mathbf{k}') + \frac{z^3}{2} \sum_{\mathbf{k}'} \sum_{\mathbf{k}''} u_3(\mathbf{k}_1, \mathbf{k}_2, \mathbf{k}_3) \; u_1(\mathbf{k}') u_1(\mathbf{k}'') + ... \right]. \tag{84}$$

Now, if we introduce the energy shift $\Delta(\mathbf{k})$ by the relation:

$$\rho_{\mathbf{k}} = z\ u_1(\mathbf{k}) \times \mathrm{e}^{-\beta\Delta(\mathbf{k})} \tag{85}$$

we obtain:

$$\mathrm{e}^{-\beta\Delta(\mathbf{k})} = 1 + z\sum_{\mathbf{k}'} u_2(\mathbf{k}_1,\mathbf{k}_2)\ u_1(\mathbf{k}') + \frac{z^2}{2}\sum_{\mathbf{k}'}\sum_{\mathbf{k}''} u_3(\mathbf{k}_1,\mathbf{k}_2,\mathbf{k}_3)\ u_1(\mathbf{k}')u_1(\mathbf{k}'') + ... \tag{86}$$

In this relation, we express the energy shift $\Delta(\mathbf{k})$ as a function of a series in power of the populations $z\,u_1(\mathbf{k})$ of the ideal gas; but if we write:

$$\mathrm{e}^{-\beta\Delta(\mathbf{k})} = 1 + \sum_{\mathbf{k}'} u_2(\mathbf{k}_1,\mathbf{k}_2)\ \mathrm{e}^{\beta\Delta(\mathbf{k}')}\ \rho_{\mathbf{k}'} + \frac{1}{2}\sum_{\mathbf{k}'}\sum_{\mathbf{k}''} u_3(\mathbf{k}_1,\mathbf{k}_2,\mathbf{k}_3)\mathrm{e}^{\beta\left[\Delta(\mathbf{k}')+\Delta(\mathbf{k}'')\right]}\ \rho_{\mathbf{k}'}\rho_{\mathbf{k}''} + ... \tag{87}$$

we obtain another expression where only the actual populations $\rho_{\mathbf{k}'}$ play a role, and from which the variable z has now disappeared. Finally, it is sufficient to take the logarithm of the right hand side of this series to obtain the expression of the energy shift $\Delta(\mathbf{k})$ as a function of the populations as well as all the other energy shifts $\Delta(\mathbf{k}')$.

In the MIME approximation, the interactions constants u_2, u_3, etc. factorize out of the sums, the energy shift becomes a constant Δ that is independent of $\mathbf{k}$, and one merely obtains:

$$\mathrm{e}^{-\beta\Delta} = 1 + u_2\,\mathrm{e}^{\beta\Delta}\,N + \frac{u_3}{2}\,\mathrm{e}^{2\beta\Delta}\,N^2 + ... \tag{88}$$

where $N \equiv \langle N\rangle$ is the mean total number of particles (the trace of ρ_I). This equation provides an implicit equation between the energy shift Δ and the density $\rho = N/\mathcal{V}$ (since u_2 is proportional to the inverse volume, u_3 to the square of this inverse volume, etc.) From this result, one can expand the energy shift in powers of the density:

$$\Delta = u_2\ N + u_3'\ N^2 + u_4'\ N^3 + ... \tag{89}$$

where the new coefficients u_3', u_4', ... can be calculated step by step by inserting this relation into (88); here again, the first term in the right hand side of (89) corresponds to the mean-field, and the following terms to density corrections. We note the similarity between this result and the usual elimination of z between the two z-expansions of the pressure and the density, which provides the equation of state, where only the actual density of the system appears. We also remark that, in general, the energy shift has a contribution that is linear in density, which can be called mean-field, but also higher order density terms (density corrections to the mean-field).

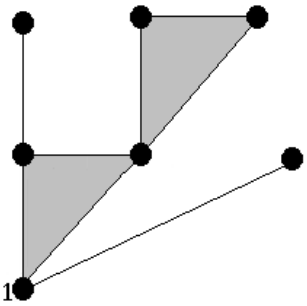

Fig. 7. An example of a diagram including irreducible parts $\overline{U}_3^{\mathrm{Irr.}}$ of the three particle Ursell operator U_3, symbolized by triangles, in addition to straight lines representing the $\overline{U}_2$'s. Such diagrams contribute to a tern in the energy shift which is quadratic in ρ_I.

Appendix C

We have defined in Section 3.2 the reducible part $\overline{U}_l^{\mathrm{R}}(1,2,...,l)$ of any Ursell operator $\overline{U}_l(1,2,...l)$ in terms of "trees" made of chains of $\overline{U}_2$ operators. For instance, the Ursell operator of order $l = 3$ then becomes the sum of a tree-reducible part and of an irreducible part:

$$\overline{U}_3(1,2,3) = \overline{U}_3^{\mathrm{R}}(1,2,3) + \overline{U}_3^{\mathrm{Irr.}}(1,2,3). \tag{90}$$

In this appendix, we sketch how the notion of reducibility could be generalized: the irreducible part $\overline{U}_3^{\mathrm{Irr.}}$ could be used, exactly as $\overline{U}_2$, as a starting point to define a "$\overline{U}_3$-reducible" part of all operators $\overline{U}_l$ with $l \geq 4$ in terms of products of $\overline{U}_2$'s and $\overline{U}_3^{\mathrm{Irr.}}$'s.

The basic idea is to build trees, not only with lines that represent $\overline{U}_2$'s, but also with triangles that represent $\overline{U}_3^{\mathrm{Irr.}}$'s. Figure 7 shows an example of such a tree: at each branching point, one may now connect either lines, or one corner of a triangle; in the latter case, the two other corners can be used as starting points in order to extend the branch further, with any product of $\overline{U}_2$'s and $\overline{U}_3^{\mathrm{Irr.}}$'s. One difference is that, because each $\overline{U}_3^{\mathrm{Irr.}}$, once added, introduces two new possible branching points (instead of a single one for a $\overline{U}_2$), the question arises as to which one is represented first in the clockwise order; it is easy to see that this introduces a 1/2 factor per $\overline{U}_3^{\mathrm{Irr.}}$ contained in the diagram into the corresponding weight. Otherwise, not much is changed, provided of course all branching factors (including those resulting from $\overline{U}_3^{\mathrm{Irr.}}$'s) are included in the weight; in other words, in formula (28), a factor $(1/2)^{n_3}$ is added (where n_3 is the number of $\overline{U}_3^{\mathrm{Irr.}}$'s), and the ramification factors r_i now include the effect of $\overline{U}_3^{\mathrm{Irr.}}$'s. This being done, the property of self similarity appears again in the series, and the essence of the reasoning still holds with relatively minor changes.

Finally, one is led to the introduction of an exponential:

$$\mathrm{e}^{-\beta\Delta(1)} \tag{91}$$

where $\Delta(1)$ would now be given by the sum:

$$-\beta\Delta(1) = \mathrm{Tr}_2\left\{\overline{U}_2(1,2)\rho_I(2)\right\} + \mathrm{Tr}_{2,3}\left\{\frac{1}{2!}\overline{U}_3^{\mathrm{Irr.}}(1,2,3)\rho_I(2)\rho_I(3)\right\}\cdot \quad (92)$$

In other words, the energy shift would no longer be proportional to the single particle density operator, but would contain a term that is quadratic in ρ_I. Similarly, one can expect that the irreducible part $\overline{U}_4^{\mathrm{Irr.}}$ of $\overline{U}_4$ would lead to a contribution to the energy shift that is cubic in ρ_I, and so on. We have not yet performed these calculations.

References

1. L.P. Kadanoff, G. Baym, *Quantum Statistical Mechanics* (Benjamin, 1962).
2. A.A. Abrikosov, L.P. Gorkov, I.E. Dzyaloshinski, *Methods of Quantum Field Theory in Statistical Physics* (Dover, 1963).
3. A.L. Fetter, J.D. Walecka, *Quantum Theory of Many-Particle Systems* (McGraw Hill, 1971).
4. P. Grüter, F. Laloë, J. Phys. **5**, 181 (1995).
5. P. Grüter, F. Laloë, J. Phys. **5**, 1255 (1995).
6. M. Holzmann, P. Grüter, F. Laloë, Eur. Phys. J. B **10**, 739 (1999).
7. J.E. Mayer, M. Goeppert Mayer, *Statistical Mechanics*, 2nd edn. (Wiley, 1975).
8. H.D. Ursell, Proc. Camb. Phil. Soc. **23**, 685 (1927).
9. G.E. Uhlenbeck, G.W. Ford, *Lectures in Statistical Mechanics* (American Mathematical Society, 1962).
10. J.P. Hansen, I.R. McDonald, *Theory of Simple Liquids*, 2nd edn. (Academic Press, 1986) Chap. 4.
11. J.E. Mayer, M. Goeppert Mayer, loc. cit. p. 258.
12. J.P. Hansen, I.R. McDonald, loc. cit. p. 91.
13. T. Morita, K. Hiroike, Prog. Theor. Phys. **25**, 537 (1961).
14. C. de Dominicis, J. Math. Phys. **3**, 983 (1962) and **4**, 255 (1963).
15. N.G. Van Kampen, Physica **27**, 783 (1961).
16. W.J. Mullin, Am. J. Physics **40**, 1473 (1972).
17. T.D. Lee, C.N. Yang, Phys. Rev. **87**, 404 (1952).
18. M. Holzmann, Ph.D. thesis, Paris (2000).
19. P. Grüter, F. Laloë, A.E. Meyerovich, W.J. Mullin, J. Phys. I France **7**, 485 (1997).
20. G. Baym, J.P. Blaizot, M. Holzmann, F. Laloë, D. Vautherin, Phys. Rev. Lett. **83**, 1703 (1999).
21. B. Kahn, G.E. Uhlenbeck, Physica **5**, 399 (1938).